Proc. Natl. Acad. Sci. USA
Vol. 89, pp. 4427–4431, May 1992
Chemistry

On the structure of the nickel/iron/sulfur center of the carbon monoxide dehydrogenase from *Rhodospirillum rubrum*: An x-ray absorption spectroscopy study

(Ni carbon monoxide dehydrogenase/*Rhodospirillum rubrum*/edge and extended x-ray absorption fine structure spectroscopy/Ni active site)

GRACE O. TAN*, SCOTT A. ENSIGN†‡, STEFANO CIURLI§, MICHAEL J. SCOTT§, BRITT HEDMAN¶, RICHARD H. HOLM§, PAUL W. LUDDEN†, Z. RICHARD KORSZUN‖, PHILIP J. STEPHENS**, AND KEITH O. HODGSON*††

*Department of Chemistry, Stanford University, Stanford, CA 94305; †Department of Biochemistry, University of Wisconsin, Madison, WI 53706; §Department of Chemistry, Harvard University, Cambridge, MA 02138; ¶Stanford Synchrotron Radiation Laboratory, Stanford University, SLAC, Bin 69, P.O. Box 4349, Stanford, CA 94309; ‖Department of Chemistry, University of Wisconsin-Parkside, Kenosha, WI 53141; and **Department of Chemistry, University of Southern California, Los Angeles, CA 90089

Contributed by Richard H. Holm, January 17, 1992

ABSTRACT **The nickel/iron/sulfur center of the carbon monoxide dehydrogenase (carbon monoxide:(acceptor)oxidoreductase; EC 1.2.99.2) enzyme from *Rhodospirillum rubrum* (*Rr*-CODH) was studied by x-ray absorption spectroscopy at the Ni K edge. Extended x-ray absorption fine structure data show that the first Ni coordination shell consists of 2 S atoms at 2.23 Å and 2–3 N/O atoms at 1.87 Å. The edge structure indicates a distorted tetrahedral or five-coordinate Ni environment in both oxidized and reduced *Rr*-CODH. By comparing second-shell extended x-ray absorption fine structure data of *Rr*-CODH to that of $(Et_4N)_3[NiFe_3S_4(SEt)_4]$, a cubane-type cluster, it was clearly established that Ni in the *Rr*-CODH center is not involved in the core of a $NiFe_3S_4$ cubane cluster. One model consistent with the results is a mononuclear Ni^{2+} site, bridged by S-Cys or sulfide to one or both of the Fe_4S_4 clusters of the enzyme, with the remaining coordination sites occupied by additional S-Cys or N/O-liganding amino acid residues.**

The metabolic pathways of certain bacteria involve conversion of CO to CO_2 catalyzed by a Ni-containing enzyme, carbon monoxide dehydrogenase [CODH; carbon-monoxide: (acceptor)oxidoreductase; EC 1.2.99.2], now purified from several anaerobes (1–12). Some of these enzymes effect the synthesis of acetyl coenzyme A by means of the Wood pathway (13, 14). Recent extended x-ray absorption fine structure (EXAFS) and x-ray absorption spectroscopy (XAS) edge studies of the CO-free, electron paramagnetic resonance-silent form of CODH from *Clostridium thermoaceticum* indicate a NiS_4 (15) or $\approx NiS_2(O/N)_2$ (16) coordination environment with distorted square-planar or pyramidal geometry (16). EXAFS further suggests that an Fe–S cluster may be nearby (15). The CODH from *Rhodospirillum rubrum* (*Rr*-CODH) is a simpler enzyme (62-kDa monomer, 1 Ni and 8 Fe/S) that only oxidizes CO (8, 9). Isotopically induced electron paramagnetic resonance line-broadening suggests that Ni is covalently coupled to one or both Fe_4S_4 clusters in *Rr*-CODH and in other enzymes as well (17–20). The possibility of an $NiFe_3S_4$ cubane-type cluster has been recognized (20), and alternative models exist in which Ni is bridged to Fe–S centers. Elucidation of the Ni-site structure is essential to understanding its role in catalysis. Toward that end, we report Ni K-edge XAS results for *Rr*-CODH.

The publication costs of this article were defrayed in part by page charge payment. This article must therefore be hereby marked "*advertisement*" in accordance with 18 U.S.C. §1734 solely to indicate this fact.

MATERIALS AND METHODS

Sample Preparations. *Rr*-CODH was purified and assayed as described (21). Purified *Rr*-CODH had a specific activity of 5200 μmol of CO oxidized per min·mg and contained 1.2 Ni and 8.1 Fe per mol of enzyme as determined by plasma emission spectroscopy. *Rr*-CODH samples were prepared for spectroscopic studies in an anaerobic glove box [Vacuum Atmospheres (Hawthorne, CA) Dri-Lab glove box model HE-493] containing an N_2 atmosphere with <1 ppm O_2. *Rr*-CODH samples in 100 mM Mops buffer, pH 7.5, were oxidized with indigo carmine as described (22) and were concentrated to 1.25 mM in a collodion ultrafiltration apparatus (Schleicher & Schuell). Some of the concentrated protein sample was reduced by adding sodium dithionite (5 mM final concentration dithionite). The oxidized and reduced samples were loaded into ≈140 μl XAS lucite cells (23 × 2 × 3 mm) with Kapton windows and frozen in liquid N_2. During the XAS experiments, no changes in the Ni x-ray absorption edge energy or shape were seen, indicating a lack of photoreduction processes, which have sometimes been observed, particularly for certain Fe- and Cu-containing metalloproteins.

Synthetic compounds were synthesized as described in the literature (24–30). They were run as finely ground solids, which had been diluted with boron nitride and pressed into pellets of 1-mm thickness and which were supported by an Al spacer and enclosed by Mylar windows.

Data Collection. Nickel K-edge x-ray absorption data for oxidized *Rr*-CODH (edge and EXAFS) were collected at the Brookhaven National Synchrotron Light Source on unfocused bending magnet beam line X19A (2.5 GeV, 92–185 mA) by using a Si(220) double-crystal monochromator. Reduced *Rr*-CODH edge and EXAFS and synthetic compound edge and EXAFS data were collected at the Stanford Synchrotron Radiation Laboratory. Protein data were measured at 10 K in fluorescence mode by using a 13-element Ge solid-state detector array (23) windowed on the Ni K_α signal. Compound data were measured at 4–10 K in transmission mode. All edge data were measured on unfocused beam lines with 1-mm vertical monochromator entrance slit. The protein data and that of compounds $(Et_4N)_2[NiFe_3S_4(PPh_3)(SEt)_3]$ (compound

Abbreviations: XAS, x-ray absorption spectroscopy; EXAFS, extended x-ray absorption fine structure; CODH, carbon monoxide dehydrogenase; *Rr*-CODH, CODH from *Rhodospirillum rubrum*.

‡Present address: Department of Botany and Plant Pathology, Oregon State University, Corvallis, OR 97331.
††To whom reprint requests should be addressed.

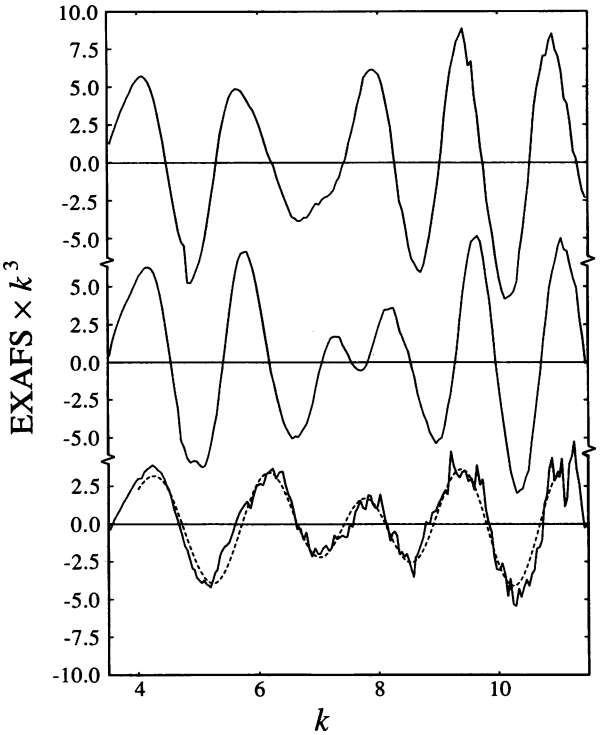

FIG. 1. Comparison of EXAFS*k^3 data (vs. k) for $(Et_4N)_3[NiFe_3S_4(SEt)_4]$ (compound 2) (top trace), $(Et_4N)_2[NiFe_3S_4(PPh_3)(SEt)_3]$ (compound 1) (middle trace), and oxidized *R. rubrum* CODH (bottom trace). ---, Best (N+S) fit.

1; ref. 24), $(Et_4N)_3[NiFe_3S_4(SEt)_4]$ (compound 2; S.C., P. K. Ross, M.J.S., S.-B. Yu, and R.H.H., unpublished work), and Ni[1,5-bis(mercaptoethyl)-1,5-diazacyclooctane]* (25) were collected on beam line 7-3, $(Bu_4N)_2$[Ni(maleonitrile dithiolate)$_2$]* (26) and $(Ph_4P)_2[Ni(SPh)_4]$* (27) on beam line 2-3, and $Ni[S_2P(OMe)_2]_2$(2,9-Me_2-1,10-phenanthroline) (28) on beam line 4-2. EXAFS data for $[Ni(ethylendiamine)_3]Cl_2$* {ref. 29; the crystal structure for this compound is not known; the Ni-N distance used is from $[Ni(en)_3]SO_4$} and $Ni(S_2CNEt_2)_2$ (30) were collected on beam lines 2-3 and 7-3, respectively (compounds marked with * were measured by R. A. Scott, University of Georgia). All data were collected under dedicated conditions (3.0 GeV, 7-60 mA) by using a Si(220) double-crystal monochromator.

Data Analysis. Data were reduced and analyzed as reported (31, 32). Energy calibration was done by using Ni foil as an internal standard, assigning the first inflection point of the Ni K absorption edge at 8331.6 eV (33). The *Rr*-CODH EXAFS data (Fig. 1) consist of an average of 16 scans from 11 Ge detector elements. Due to a monochromator glitch at k of 12.8 Å^{-1}, the data range used in this preliminary report is truncated at 11.5 Å^{-1}. The normalized background-subtracted data were converted to k space by assuming a threshold energy of 8350 eV. Curve-fitting techniques were applied by using empirical phase and amplitude parameters for Ni–*X* scattering pairs from these compounds: Ni–N, $[Ni(ethylenediamine)_3]Cl_2$ (29); Ni–S, $Ni(S_2CNEt_2)_2$ (30); Ni–Fe, compound 1 (24). The cluster anions of compounds 1 and 2 contain the $NiFe_3S_4$ cubane-type core below; mean Ni–S and Ni–Fe bond distances obtained for compound 1 from crystallography (24) are indicated.

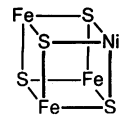

Ni—S 2.262(6) Å

Ni—Fe 2.69(2) Å

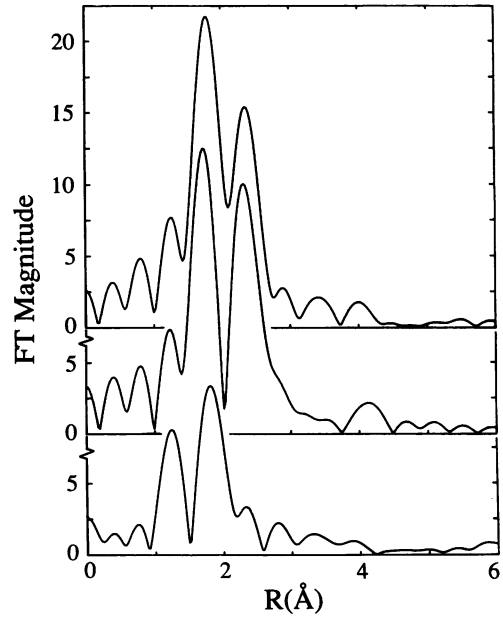

FIG. 2. Comparison of Fourier transforms (FT) of EXAFS data (k range of 3.5–11.5 Å^{-1}) of $(Et_4N)_3[NiFe_3S_4(SEt)_4]$ (compound 2) (top trace) and $(Et_4N)_2[NiFe_3S_4(PPh_3)(SEt)_3]$ (compound 1) (middle trace), and oxidized *Rr*-CODH (bottom trace).

RESULTS AND DISCUSSION

The Fourier transform of the EXAFS data for oxidized *Rr*-CODH over the k range of 3.5–11.5 Å^{-1} is shown in Fig. 2 (bottom trace). Curve fitting was done on data from Fourier-filtered first- and second-shell contributions individually as well as on data covering both regions. All fits were done for the data range k = 4–11 Å^{-1}. The first shell of *Rr*-CODH showed a strong beat, and we found that reasonable fit results could only be obtained using data Fourier-filtered over the wide region of R = 0.85–2.25 Å (i.e., including the first two major peaks in Fig. 2) and fitting with more than one shell of atoms. Two-wave fits, N+S, N+N′, and S+S′, were thus performed. Of these, N+S gave the best fit results and the most physically plausible values for distance, coordination number, and relative Debye–Waller factors. As summarized in Table 1, the first coordination shell consists of 2–3 N atoms at 1.87 Å and 2 S atoms at 2.23 Å.‡‡ In contrast, only one S shell was needed to give a reasonable fit to the first shell (R = 1.35–2.15 Å) of cubane compound 2 (Table 1; the Fourier transform is shown in Fig. 2, top trace). As seen in Table 1, fits with fixed coordination numbers and varied Debye–Waller factors gave results quite similar to those where only the coordination number was varied. However, the coordination number for S in the cubanes (using the Ni–S parameters described above) was lower than expected, both for narrow and wide-range filters.

Fig. 2 shows a large difference in the intensity of the second-shell peak (≈2.35 Å); that of *Rr*-CODH is much lower and only about twice above noise level as compared with that for the cubanes. Fits to the combined first and second shells

‡‡In parallel, independent of the Ni K edge protein XAS data presented here, XAS data from the same source of protein were also measured at the National Synchrotron Light Source and are being analyzed by Z.R.K. Preliminary results from the analysis of these data by using different phase and amplitude parameters (theoretical) agree reasonably well with our results. Fits of the Ni K edge EXAFS show Ni–S and Ni–N/O coordination similar to those reported here and a distinct absence of a short Ni–Fe interaction. Further, edge and EXAFS data were measured at the Fe K edge. These data will be reported elsewhere.

Table 1. Summary of EXAFS curve-fitting results

	R_N, Å	CN_N	$\Delta\sigma^2_N$*	R_S, Å	CN_S	$\Delta\sigma^2_S$*	R_{Fe}, Å	CN_{Fe}	$\Delta\sigma^2_{Fe}$*	F†
Ni CODH	1.87	2.7	(0)	2.23	1.8	(0)				0.529
Ni CODH	1.86	(2)	−0.0029	2.22	(2)	0.0009				0.487
Ni CODH‡	1.86	5.5	(0)	2.07	7.6	(0)				0.659
Ni CODH§	1.62	0.5	(0)	2.23	1.4	(0)				0.625
Ni cubane¶				2.26	2.6	(0)				0.333
Ni CODH	1.87	2.7	(0)	2.23	1.8	(0)	2.93	0.06	(0)	0.630
Ni CODH	1.86	(2)	−0.0034	2.22	(2)	0.0005	2.73	(1)	0.0136	0.502
Ni cubane¶				2.25	2.7	(0)	2.74	2.6	(0)	0.521
Ni cubane¶				2.26	(3)	0.0007	2.74	(3)	0.0011	0.499

Errors in distance (±0.03 Å) and coordination number (±25%) are estimated from variance of fitting results between true values from models of known structure. Values enclosed in parentheses were fixed during the refinements. *R*, distance, *CN*, coordination number.

*Relative Debye–Waller term, expressed as σ^2 (sample) − σ^2 (reference), where reference is $[Ni(ethylenediamine)_3]Cl_2$ for Ni–N, $Ni(S_2CNEt_2)_2$ for Ni–S, and compound 1 for Ni–Fe.

†F is a goodness-of-fit criterion defined by $F = [\Sigma\, k^6(\text{data} - \text{fit})^2/(\text{number of points})]^{1/2}$.

‡These are fit results using N+N′ waves (no S wave).

§These are fit results using S+S′ waves (no N wave).

¶Compound 2.

of *Rr*-CODH and compound 2 (EXAFS filtered over 0.85–3.15 Å and 1.30–2.85 Å, respectively) showed that although 2.6 Fe at 2.74 Å was found for the cubane (agreeing well with the expected value of 3 Fe atoms), <0.1 Fe (at 2.93 Å) was found for *Rr*-CODH when the Debye–Waller factor was kept fixed. Alternatively, when 1 Fe atom was assumed (fixed) and the Debye–Waller factor was varied, a distance of 2.73 Å was found but with an unreasonably high relative Debye–Waller factor. We therefore conclude that the active site of *Rr*-CODH does not include a rigid $NiFe_3S_4$ cubane cluster. A summary of the fitting results is given in Table 1, and graphical comparisons are shown in Figs. 1 and 3.

The Ni K x-ray absorption edge spectrum of oxidized *Rr*-CODH is shown in Fig. 4. Included for comparison are Ni edge spectra of several S- and N,S-coordinated Ni complexes of planar (top traces), distorted five-coordinate and tetrahedral (middle traces), and $NiFe_3S_4$-cubane (bottom traces) geometry. Ni K-edge features show systematic trends that have been interpreted to be diagnostic of certain coordination geometries (16, 34, 35). The relatively weak preedge feature around 8333 eV is generally accepted to derive from a $1s \rightarrow 3d$ transition. This transition is formally forbidden, but it can derive intensity by $d \rightarrow p$ admixture in noncentrosymmetric molecules. Assignment of the next higher energy feature on the rising part of the Ni absorption edge (around 8338 eV) is less definitive, but most likely it derives from $1s \rightarrow 4p$ character plus a shakedown component. Edge comparisons from complexes of known structure indicate that this "$1s \rightarrow 4p$" transition is strong and quite well resolved in square-planar complexes. Less well-resolved and lower-intensity transitions are observed for five-coordinate pyramidal complexes, whereas the transitions are much weaker or absent for typical tetrahedral and trigonal bipyramidal geometries. As with all x-ray absorption edges, care must be taken in deriving formal charge on the metal because the absolute energies vary with both formal oxidation state as well as the relative electronegativity of the ligands. Caution must also be exercised in comparing edges from different studies where energy resolutions differ with the specific monochromator and defining slit size used.

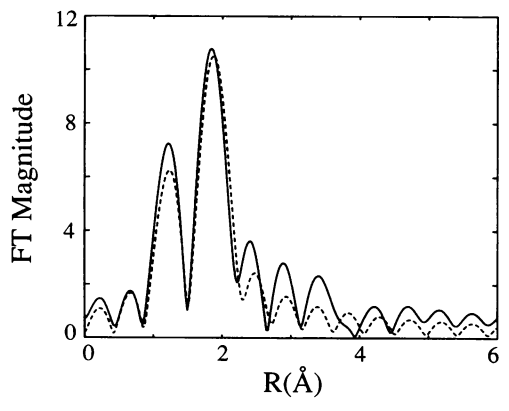

FIG. 3. Comparison of Fourier transforms (FT) (over k range of 4.0–11.0 $Å^{-1}$) of *Rr*-CODH data (——) and of the best (N+S) fit (– – –).

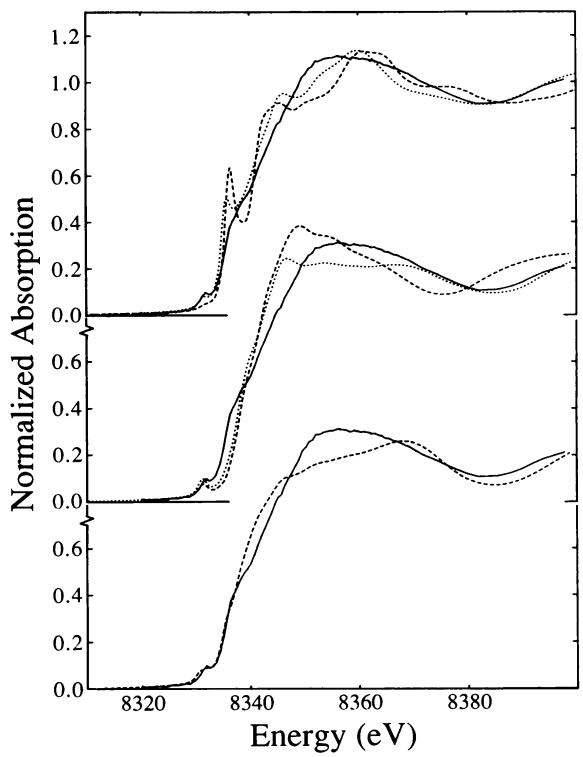

FIG. 4. Comparisons of the edge of oxidized *Rr*-CODH (—— in all plots) with edges of various Ni compounds. (Top traces) Comparison with $(Bu_4N)_2[Ni(maleonitrile\ dithiolate)_2]$ (26) (– – –, planar Ni–S_4 ligation) and Ni[1,5-bis(mercaptoethyl)-1,5-diazacyclooctane] (25) (· · ·, planar Ni–N_2S_2 ligation a with slight tetrahedral distortion). (Middle traces) Comparison with $Ni[S_2P(OMe)_2]_2$(2,9-Me_2-1,10-phenanthroline) (28) (– – –, distorted trigonal bipyramidal Ni–N_2S_3 ligation) and $(Ph_4P)_2[Ni(SPh)_4]$ (27) (· · ·, tetrahedral Ni–S_4 ligation). (Bottom traces) Comparison with the cubane cluster 1 (24) (– – –, distorted tetrahedral Ni–S_3P ligation).

From spectra of others (16, 34, 35) as well as those recorded by us, several conclusions can now be drawn about the Ni site in *Rr*-CODH. (*i*) The edge spectra for oxidized and reduced *Rr*-CODH (data not shown) are very nearly superimposable, thus indicating that the additional electron does not reside in primarily Ni-derived orbitals and that there is no significant structural rearrangement upon oxidation/reduction.§§ (*ii*) Each edge spectrum in Fig. 4, except for the planar NiS_4 complex, shows a partially resolved $1s \rightarrow 3d$ transition at ≈8332 eV. The intensity of this transition for *Rr*-CODH is higher than would be expected for planar NiS_4 coordination (compare Fig. 4 top trace) and is more consistent with distorted five-coordinate or tetrahedral coordination and a noncentric Ni environment (compare Fig. 4 middle and bottom traces). (*iii*) The intensity of the higher energy feature at ≈8337 eV (assigned to a "$1s \rightarrow 4p$" transition) is lower for *Rr*-CODH than typically found in planar Ni complexes and is more intense than that expected of pure tetrahedral coordination. Interestingly, the shape and early rise of the Ni edges of *Rr*-CODH and compound 1 are quite similar, consistent with both having the Ni^{2+} oxidation state. {A description of the electronic structure of the $[NiFe_3S_4]^{1+}$ core comes from a combination of electron paramagnetic resonance, Mössbauer, and structural studies (24) and suggests Ni and average Fe oxidation states of +2 and +2.33, respectively. The $[NiFe_3S_4]^{1+}$ core is best described from these studies as an S = 5/2 $[Fe_3S_4]^{1-}$ cluster fragment antiferromagnetically coupled to an S = 1 Ni^{2+} ion in a tetrahedral or pseudotetrahedral geometry.} Significant differences in the edges of *Rr*-CODH and compound 1 do occur above ≈8337 eV, but quantitative interpretation must await detailed calculation of both the bound/continuum region and multiple scattering effects. Overall, the *Rr*-CODH Ni edge indicates distorted four- or five-coordinate geometry about Ni and, thus, is consistent with the EXAFS results.

In summary, EXAFS results at the Ni K edge for *R. rubrum* CODH clearly preclude involvement of Ni in the core of a rigid $NiFe_3S_4$ cubane cluster. This conclusion is strongly reinforced by EXAFS analysis of an authentic, well-characterized $NiFe_3S_4$ complex (compound 2), using the same phase and amplitude parameters as in the analysis of *Rr*-CODH. Rather, the results reveal a mononuclear Ni atom in *Rr*-CODH with a significant degree of sulfur coordination plus several lower-Z (N,O) ligands completing the first coordination shell. Edge features indicate that a planar four-coordinate structure is unlikely and point to a distorted noncentric tetrahedral or five-coordinate Ni environment in oxidized and reduced *Rr*-CODH. As for *C. thermoaceticum* CODH (15, 16), no firm evidence is found for the presence of Ni–Fe interactions. One model consistent with our XAS results is a mononuclear Ni^{2+} site, bridged by S-Cys or sulfide to one or both Fe_4S_4 clusters with the remaining coordination sites being occupied by additional S-Cys or N/O-liganding amino acids.

It should be noted that EXAFS analysis *per se* cannot normally identify a specific type of amino acid with a given ligand (for example, determining that the S ligand comes from S-Cys vs. S-Met). In special cases, with high-quality data over wider *k* range, certain amino acids with rigid arrangements of outer shell atoms (such as imidazole) have relatively large multiple scattering signals that give rise to "signatures" that can be detected in EXAFS data. For the present *Rr*-CODH data, there are no clear indications of such effects. Further, based on known Ni^{2+}–S distances, the Ni–S distances in *Rr*-CODH are consistent with either S-Cys or S-Met ligation.

§§In contrast to the Ni edges for oxidized and reduced *Rr*-CODH, changes are seen in the region of the Fe absorption edges for the same samples. These results will be discussed in detail elsewhere.

It is quite possible that EXAFS analysis would not be able to readily detect the presence of longer-distance Ni–Fe interactions as a result of decreased structural rigidity and thus increased thermal damping (as compared, for example, to the very ordered and rigid environment of Ni in a cubane structure). In cases where the metal–metal pairwise Debye–Waller factor is small (generally cases where the metal pair is rigidly bridged), strong contributions to the EXAFS signal are normally found. In contrast, for nonbridged or weakly bridged systems, the metal–metal contribution may not be clearly observable, and even if it is, interpretation may be complicated by scattering from C/N atoms in the outer shells of ligands that can mimic the metal–metal contribution (36–38).

If present in *Rr*-CODH, a Ni–Fe distance from mononuclear Ni^{2+} to a Fe_4S_4 cluster would thus likely be greater than ≈3 Å; EXAFS data of improved S/N over a wider range of *k* could more definitively address this question. A model in which Ni is S-bridged to one or two Fe_4S_4 clusters is also consistent with the apparent electronic coupling of the Ni and Fe–S sites (10).

We thank Prof. Robert A. Scott for kindly sharing with us the XAS data of several Ni compounds. The data were collected at the Stanford Synchrotron Radiation Laboratory and the National Synchrotron Light Source, Brookhaven, which are supported by the Department of Energy, Office of Basic Energy Sciences, Divisions of Chemical Sciences and Materials Sciences. Stanford Synchrotron Radiation Laboratory is also supported in part by the National Institutes of Health, Biomedical Resource Technology Program, Division of Research Resources (RR-01209) and by the Department of Energy Offices of Health and Environmental Research. This research was supported by National Institutes of Health Grant GM 28856 (to R.H.H.), Department of Energy Grant DE-FG02-87ER13691 (to P.W.L.), National Institutes of Health Grant GM 41822 (to Z.R.K.), and National Science Foundation Grant CHE 88-17702 (to K.O.H.). S.A.E. was supported by National Institutes of Health Training Grant 5T32GM07215-14 and by a graduate fellowship from the College of Agricultural and Life Sciences.

1. Drake, H. L., Hu, S.-I. & Wood, H. G. (1980) *J. Biol. Chem.* **255,** 7174–7180.
2. Ragsdale, S. W., Clark, J. E., Ljungdahl, L. G., Lundie, L. L. & Drake, H. L. (1983) *J. Biol. Chem.* **258,** 2364–2369.
3. Diekert, G. B. & Thauer, R. K. (1978) *J. Bacteriol.* **136,** 597–606.
4. Ragsdale, S. W., Ljungdahl, L. G. & DerVartanian, D. V. (1983) *J. Bacteriol.* **155,** 1224–1237.
5. Grahame, D. A. & Stadtman, T. C. (1987) *J. Biol. Chem.* **262,** 3706–3712.
6. Krzycki, J. A. & Zeikus, J. G. (1984) *J. Bacteriol.* **158,** 231–237.
7. Terlesky, K. C., Nelson, M. J. K. & Ferry, J. G. (1986) *J. Bacteriol.* **168,** 1053–1058.
8. Bonam, D. & Ludden, P. W. (1987) *J. Biol. Chem.* **262,** 2980–2987.
9. Ensign, S. A., Bonam, D. & Ludden, P. W. (1989) *Biochemistry* **28,** 4968–4973.
10. Bonam, D., McKenna, M.-C., Stephens, P. J. & Ludden, P. W. (1988) *Proc. Natl. Acad. Sci. USA* **85,** 31–35.
11. Bonam, D., Murrell, S. A. & Ludden, P. W. (1984) *J. Bacteriol.* **159,** 693–699.
12. Abbanat, D. R. & Ferry, J. G. (1990) *J. Bacteriol.* **172,** 7145–7150.
13. Ragsdale, S. W. (1991) *Crit. Rev. Biochem. Mol. Biol.* **26,** 261–300.
14. Wood, H. G., Ragsdale, S. W. & Pezacka, E. (1986) *Biochem. Int.* **12,** 421–440.
15. Bastian, N. R., Diekert, G., Niederhoffer, E. C., Teo, B.-K., Walsh, C. T. & Orme-Johnson, W. H. (1988) *J. Am. Chem. Soc.* **110,** 5581–5582.
16. Cramer, S. P., Eidsness, M. K., Pan, W.-H., Morton, T. A., Ragsdale, S. W., DerVartanian, D. V., Ljungdahl, L. G. & Scott, R. A. (1987) *Inorg. Chem.* **26,** 2477–2479.

17. Ragsdale, S. W., Ljungdahl, L. G. & DerVartanian, D. V. (1983) *Biochem. Biophys. Res. Commun.* **115,** 658–665.
18. Ragsdale, S. W., Wood, H. G. & Antholine, W. E. (1985) *Proc. Natl. Acad. Sci. USA* **82,** 6811–6814.
19. Terlesky, K. C., Barber, M. J., Aceti, D. J. & Ferry, J. G. (1987) *J. Biol. Chem.* **262,** 15392–15395.
20. Stephens, P. J., McKenna, M.-C., Ensign, S. A., Bonam, D. & Ludden, P. W. (1989) *J. Biol. Chem.* **264,** 16347–16350.
21. Ensign, S. A., Hyman, M. R. & Ludden, P. W. (1989) *Biochemistry* **28,** 4973–4979.
22. Ensign, S. A., Campbell, M. J. & Ludden, P. W. (1990) *Biochemistry* **29,** 2162–2168.
23. Cramer, S. P., Tench, O., Yocum, M. & George, G. N. (1988) *Nucl. Instr. Methods Phys. Res.* **A266,** 586–591.
24. Ciurli, S., Yu, S.-B., Holm, R. H., Srivastava, K. K. P. & Münck, E. (1990) *J. Am. Chem. Soc.* **112,** 8169–8171.
25. Mills, D. K., Reibenspies, J. H. & Darensbourg, M. Y. (1990) *Inorg. Chem.* **29,** 4364–4366.
26. Kobayashi, A. & Sasaki, Y. (1977) *Bull. Chem. Soc. Jpn.* **50,** 2650–2656.
27. Swenson, D., Baenziger, N. C. & Coucouvanis, D. (1978) *J. Am. Chem. Soc.* **100,** 1932–1934.
28. Shetty, P. S. & Fernando, Q. (1970) *J. Am. Chem. Soc.* **92,** 3964–3969.
29. Mazhar-Ul-Haque, Caughlan, C. N. & Emerson, K. (1970) *Inorg. Chem.* **9,** 2421–2424.
30. Bonamico, M., Dessy, G., Mariani, C., Vaciago, A. & Zambonelli, L. (1965) *Acta Crystallogr.* **19,** 619–626.
31. Cramer, S. P. & Hodgson, K. O. (1979) *Prog. Inorg. Chem.* **15,** 1–39.
32. Cramer, S. P., Hodgson, K. O., Stiefel, E. I. & Newton, W. E. (1978) *J. Am. Chem. Soc.* **100,** 2748–2761.
33. Scott, R. A., Penner-Hahn, J. E., Doniach, S., Freeman, H. C. & Hodgson, K. O. (1982) *J. Am. Chem. Soc.* **104,** 5364–5369.
34. Eidsness, M. K., Sullivan, R. J. & Scott, R. A. (1988) in *The Bioinorganic Chemistry of Nickel*, ed. Lancaster, J. R. (VCH, New York), pp. 73–91.
35. Colpas, G. J., Maroney, M. J., Bagyinka, C., Kumar, M., Willis, W. S., Suib, S. L., Baidya, N. & Mascharak, P. K. (1991) *Inorg. Chem.* **30,** 920–928.
36. Hedman, B., Co, M. S., Armstrong, W. H., Hodgson, K. O. & Lippard, S. J. (1986) *Inorg. Chem.* **25,** 3708–3711.
37. Scott, R. A. & Eidsness, M. K. (1988) *Comments Inorg. Chem.* **7,** 235–267.
38. DeWitt, J. G., Bentsen, J. G., Rosenzweig, A. C., Hedman, B., Green, J., Pilkington, S., Papaefthymiou, G. C., Dalton, H., Hodgson, K. O. & Lippard, S. J. (1991) *J. Am. Chem. Soc.* **113,** 9219–9235.